Journal of Young Pharmacists, 2023; 15(4):629-637.
https://www.jyoungpharm.org

Original Article

Mechanistic Insights into Ipriflavone's Role in Postmenopausal Osteoporosis through Integrated Computational and *in vitro* Techniques

Anish John, Harsha Ashtekar, Dheeraj Gupta, Pankaj Kumar, Anoop Narayanan V*

NITTE (Deemed to be University), NGSM Institute of Pharmaceutical Sciences, Mangalore, Karnataka, INDIA.

ABSTRACT

Background: Postmenopausal osteoporosis affects a large percentage of the female population worldwide. Understanding the molecular pathways is critical for effective treatment. This study aimed to assess ipriflavone's efficacy in treating postmenopausal osteoporosis using computational techniques and *in vitro* evidence. **Materials and Methods:** Ligands were prepared for docking while receptors were readied via protein preparation. Molecular docking was performed to generate ligand-receptor complexes which underwent molecular dynamics simulation using GROMACS. Simulation trajectories were analyzed to gauge binding stability. Finally, ligand activity against MG-63 osteosarcoma cells was evaluated through MTT and Alizarin Red assays to measure viability and calcium uptake respectively. **Results:** The results of the study indicated that ipriflavone can modulate several genes associated with postmenopausal osteoporosis, including ESR1, ESR2, CYP19A1, LGMN, CASP3, BMP4, TNFRSF1A, and CTSK. Among these genes, ipriflavone showed the highest binding affinity with estrogen receptors (ESR1 and ESR2) with a docking score of -8.7 kcal/mol. Molecular dynamics analysis confirmed the stability of the ipriflavone complex for up to 200 ns. Pathway analysis using KEGG revealed the specific pathways modulated by ipriflavone. Furthermore, *in vitro* experiments using the MG63 cell line demonstrated that ipriflavone is non-toxic and can increase calcium uptake, indicating its potential osteogenic effect. The MTT assay supported the safety of ipriflavone treatment in MG63 cells. **Conclusion:** This study illuminates ipriflavone's anti-osteoporotic mechanism. According to this study, ipriflavone may modify estrogen receptors and treat postmenopausal osteoporosis. More *in vivo* investigations are needed to prove ipriflavone's biological potency and efficacy in a more complex physiological environment.

Keywords: Postmenopausal osteoporosis, MG63 cells, Ipriflavone, Estrogen receptor, Bone development.

Correspondence:
Dr. Anoop Narayanan V
Assistant Professor, Department of Pharmaceutics, NITTE (Deemed to be University), NGSM Institute of Pharmaceutical Sciences, Mangalore-575018, Karnataka, INDIA.
Email: anoopnarayanan@nitte.edu.in

Received: 14-08-2023;
Revised: 17-09-2023;
Accepted: 19-10-2023.

INTRODUCTION

Postmenopausal osteoporosis is a prevalent global disease, impacting approximately 200 million women worldwide. In the United States, it affects around 10 million individuals with an additional 44 million having low bone mass, making them susceptible to fractures.[1] In India, the prevalence of osteoporosis in postmenopausal women ranges from 19.3% to 57.9%, according to the reports of region and population.[2] Both women and men are affected by bone fracture-related issues around 50 years of age.[3] As a result of population expansion and ageing, it is anticipated that the total number of osteoporotic fracture cases may increase twofold by 2050.[4]

Postmenopausal osteoporosis poses a substantial health risk, increasing the susceptibility to fractures and diminishing overall well-being. Bisphosphonates, denosumab, teriparatide, HRT and ERM are therapeutic approaches for addressing postmenopausal osteoporosis. Bisphosphonates act on osteoclasts and inhibit bone resorption.[5] Denosumab, a monoclonal antibody that inhibits the RANK ligand, has also been shown to reduce the risk of fractures in postmenopausal women with osteoporosis.[6] Teriparatide, a recombinant human parathyroid hormone, has increased bone mineral density by increasing osteoblast formation and inhibiting osteoblast apoptosis.[7] Estrogen replacement therapy is one of the most effective treatments for osteoporosis. It works by slowing down bone loss and increasing bone density. However, HRT is associated with certain risks and side effects, and its use should be carefully monitored.[8] Selective Estrogen Receptor Modulators (SERMs) mimic the effects of estrogen to increase bone mineral density by down modulating the activity of osteoclasts in transforming growth factor-β3.[9] Clinical

DOI: 10.5530/jyp.2023.15.88

studies have shown that ipriflavone can significantly increase Bone Mineral Density (BMD) and decrease the risk of vertebral fractures in postmenopausal women with osteoporosis, especially when combined with calcium supplements.[10] Ipriflavone works by inhibiting bone resorption and stimulating bone formation, primarily through its effects on osteoblast and osteoclast activity.[11] However, more research is needed to understand its long-term safety and effectiveness fully.

The results indicated that ipriflavone displayed limited estrogenic activity and had the potential to interact with the estrogen receptor.[12] These findings suggest that ipriflavone might function as a Selective Estrogen Receptor Modulator (SERM), exerting estrogen-like effects on bone and other bodily tissues. This study provides important insights into the mechanism of action of ipriflavone and its potential applications in treating osteoporosis and other estrogen-related disorders.[13]

In recent drug development computational approach is used to find the responsible gene pathways involved in the disease progression and to find the possible mechanism involved to target these pathways by various drug molecules, in this regards this study is designed to evaluate the efficacy of ipriflavone in the treatment of postmenopausal osteoporosis using computational tools and *in vitro* studies like identification of genes involved in the disease and ipriflavon modulating genes, finding protein-protein interactions of common genes involved, gene ontology, KEGG pathway, molecular docking, ADME profile of drug, molecular simulation and *in vitro* alp, calcium uptake assay.

MATERIALS AND METHODS

In silico studies

Protein selection and preparation

Ipriflavon canonical SMILES were extracted from PubChem database. The proteins involved in disease progression were identified from DisGeNET database (https://www.disgenet.org/). Whereas protein targets were predicted using the Swiss target prediction (http://www.swisstargetprediction.ch/) for ipriflavone. Further, the common targets for osteoporosis and ipriflavone were taken from the Venny 2.1.0 online tool.[14-16]

Protein-Protein Interaction Data

String 11.5 (https://string-db.org/) online database was used for predicting protein interactions, including direct and indirect protein interactions. It scores each protein interaction. A higher score means a higher confidence of protein interaction. The selected intersection targets were imported into String for protein interaction analysis, and the protein interaction network was obtained with the species limited to "Homo sapiens". The protein interaction data were imported into Cytoscape (https://cytoscape.org/) to construct the PPI network and highest degree of interaction with common genes retracted from Venny 2.0.1.[17-19]

Gene Ontology (GO) and Pathway Enrichment

DAVID (https://david.ncifcrf.gov/) database integrates various types of database resources and uses the improved Fisher precision test algorithm to analyse the enrichment of gene sets. A cut off P value and False Discovery Rate (FDR)<0.05 were used to indicate statistical significance. GO annotation and KEGG PATHWAY analysis were carried out for the intersection genes. Finally, we could get the pathway maps from KEGG PATHWAY Database (https://www.kegg.jp/).[20-22]

Molecular Docking Verification

Preparation of ligand and protein

The LigPrep module was used to prepare ligands for docking. Ligands were transformed into 3D structures via ionisation, tautomerism, energy minimisation, and geometry optimisation. Further, ionisation and tautomeric states were generated in the pH range of 6.8 to 7.2 using the Epik module. The X-ray crystallographic structure of the proteins comprising co-crystalline ligand, water molecule, metal ions, and cofactors were retrieved from the protein data bank. The protein preparation wizard was used to prepare proteins. The energy minimisation of the protein was performed using the Optimised Potentials for Liquid Simulations-3 (OPLS3) force field.[23,24]

Receptor grid set to generation and Glide ligand docking

A receptor grid for protein-ligand docking was generated via the site map module. The binding site possessing the largest volume was taken under consideration to form a grid where docking is to be performed. Ipriflavone was docked into the generated grid. The docking was performed in a versatile docking mode that automatically generated conformations for each input ligand, using extra precision mode. The ligand possessing the least glide scores were utilised to visualise the protein-ligand interaction by the Glide module's XP visualiser and a 2D image of the interaction was extracted.[25,26]

MD simulation

To perform MD simulation, gromacs (https://www.gromacs.org/) ver. 2023.1 was used. The hetero atoms from complex was removed by using the UCSF chimera. The protein topology was generated by applieng CHARMM 27 force filed and the ligand topology by the swiss param portal online tool also, gestiger charges added the H. The intermediate complex was built using the editconf module of gromacs. The complex was then solvated using a triclinic box with 1 nm dimensions on all sides, utilising a TETP1 water model. The system was neutralised by adding Na+ and Cl- counter ions as required. To minimise energy, the system was subjected to steepest descent integrator with a verlet cutoff-scheme for a maximum of 55000 steps, followed by adding restrains. The system was then equilibrated using Canonical (NVT) and Isobaric (NPT) for 10 ps for two coupling

groups: protein-ligand and water-ions. A modified Berendsen thermostat (V-rescale) was used to maintain constant volume and temperature at 300 K, while a C-rescale pressure coupling algorithm was applied to maintain constant pressure at 1 bar. Particle Mesh Ewald (PME) was used for computing long-range electrostatics, coulomb, and Van der Waals with a cut-off of 1.2 nm. The LINCS algorithm was used to constrain bond length. Each complex was subjected to an MD run for 200 ns, and the coordinates and energies were saved at every 200 nanoseconds to acquire 100000 frames. The generated trajectories were analysed using the in-built gromacs utilities. The Root Mean Square Deviation (RMSD), Root Mean Square Fluctuation (RMSF), Radius of Gyration (RoG), Solvent Assessable Surface Area (SASA), and Number of hydrogen bonds were retrieved for a time span of 200 ns and visualised using QtGrace.[27-29]

Biological activity

Cells and cell culture

MG-63 cell maintenance and culture involve several key steps. Initially, a DMEM medium is prepared, supplemented with 10% FBS and 1% antibiotics. The cells are counted using an automated cell counter and then seeded onto 96 well culture plate. Feeding with fresh medium is accomplished every 2-3 days to provide nutrients for cell growth. When the cells reach 80-90% confluence, they are subcultured or passaged to maintain viability. Regular monitoring of cell growth, morphology, and contamination is essential.

MTT assay

MTT assay is a commonly used colourimetric assay to assess cell viability and proliferation. It measures the activity of mitochondrial enzymes that can convert the yellow water-soluble substrate, MTT (3-(4,5-dimethylthiazol-2-yl)-2,5-diphenyltetrazolium bromide), into a purple formazan product. The formazan formed is directly proportional to the number of viable cells in the culture.

Dissolve MTT powder in a sterile buffer or culture medium to create a concentrated MTT solution (usually 5 mg/mL). Seed the cells and allow them to adhere and grow. Treat the cells with various concentrations of ipriflavon. Remove the culture medium and replace it with a fresh medium. Add the MTT solution to each well, ensuring it is evenly distributed. Incubate the cells with MTT at 37°C for 4 hr. After the incubation, carefully remove the MTT-containing medium. The formazan crystals formed by viable cells remain insoluble. To solubilise the formazan, add a dimethyl sulfoxide to each well and gently shake the plate to dissolve the crystals fully. Transfer the dissolved formazan solution from each well into a new microplate or cuvette and measure the absorbance at a specific wavelength (usually around 570 nm) using a spectrophotometer. The absorbance is proportional to the number of viable cells present. Normalise the absorbance values to control samples and calculate the relative cell viability or proliferation based on the experimental design.[30-32]

Calcium uptake assay by Alizarin red

Calcium uptake by MG-63 cells was monitored by incubating cells in 6 well pates with test compound for 24 hr. After the incubation period, the treated cells were washed with PBS and fixed in 4% paraformaldehyde at room temperature for 20 min.

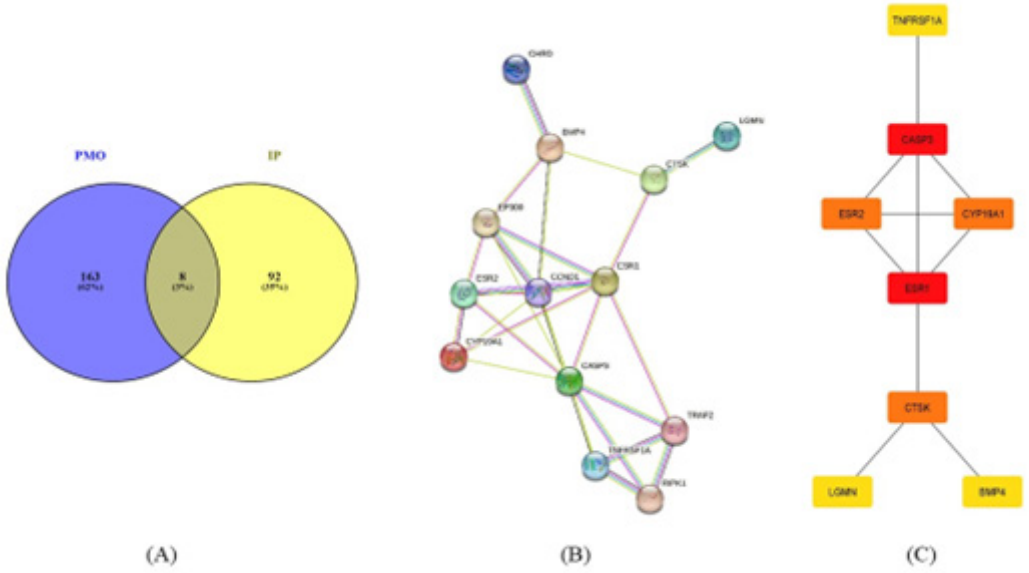

Figure 1: (A) Venny diagram of disease gene and ipriflavone compounds, (B) The protein-protein interaction from string database (PPI), (C) The common genes of ipriflavone and disease genes with its protein-protein interaction with degree segregation red is highest orange intermediate and yellow is lowest. PMO-Postmenopausal osteoporosis; IP-Ipriflavone.

The fixed cells were stained with freshly prepared alizarin red (2% aqueous, pH 4.2) and washed with PBS. The intensity of the stain uptake was used to assess the calcium accumulation and compare it with the untreated control. Alizarin red stain from the cells was extracted using 10% acetic acid and quantified at 405 nm using a multimode microplate reader.[33]

RESULTS

Targets of ipriflavone and postmenopausal osteoporosis

The Canonical SMILE of ipriflavon was retrieved from PubChem. Based on chemical structural similarity, we used SwissTarget Prediction online databases to predict their targets. A total of 201 targets were predicted for ipriflavone. For disease gene prediction, the disgenet database has a total of 171 genes for postmenopausal osteoporosis with Disgenet ID-CUI: C0029458. Based on targets of the ipriflavone and postmenopausal osteoporosis, intersection targets were got by Venny 2.0.1. eight intersection genes were found eventually, shown in Figure 1(A); details of intersection targets are described in Table 1.

Gene Ontology

GO analysis of 8 candidate targets for ipriflavone against postmenopausal osteoporosis was performed using the DAVID database to understand the relationship between functional units and their underlying significance in the biological system networks. The results were divided into three parts, including biological processes, cellular components, and molecular function, as shown in Figure 2(A). The data was generated using

Table 1: Ipriflavone targeted protein, gene and protein class related to postmenopausal osteoporosis.

Gene-ID	PDB-ID	Gene Name	Protein Class
ESR1	1A52	Estrogen receptor 1	Nuclear receptor
ESR2	1L2J	Estrogen receptor 2	Nuclear receptor
CYP19A1	3EQM	Cytochrome P450 family 19 subfamily A member 1	Enzyme
LGMN	4AW9	Legumain	Enzyme
CASP3	1CP3	Caspase 3	Enzyme
BMP4	2HQL	Bone morphogenetic protein 4	Signaling
TNFRSF1A	1FP3	TNF receptor superfamily member 1A	NA
CTSK	1ATK	Cathepsin K	Enzyme

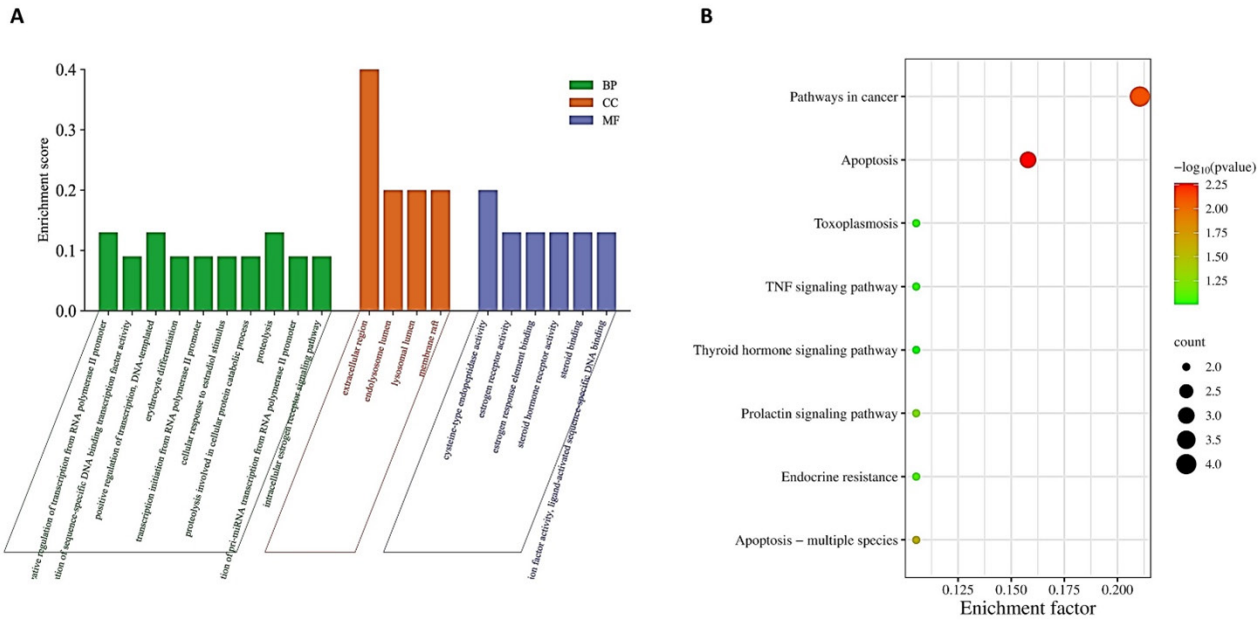

Figure 2: (A) Gene ontology enrichment analysis of biological process (green), cellular component (orange), molecular function (purple), (B) Bubble chart of KEGG pathways analysis.

the bioinformatics tool (https://www.bioinformatics.com.cn/plot_basic_GO_term_bp_cc_mf_bar_plot_046_en) depicted in Figure 2(A).

Pathway Enrichment

Rough comprehensive analysis, we obtained an integrated postmenopausal osteoporosis pathway based on our current knowledge of postmenopausal osteoporosis pathogenesis to illuminate the integral role of ipriflavone in treating postmenopausal osteoporosis. TOP 8 KEGG signaling pathways of BHD were obtained and constructed based on *p* value, as shown in Figure 2(B).

Ipriflavone-postmenopausal osteoporosis Network

Eight intersection targets were imported into the String database, and TSV text showing the interaction relationship was obtained with the addition of node interaction, as shown in Figure 1(B). This network contained 18 nodes and 53 edges. Then, the network topology analysis was applied by the software of Cytoscape 3.6.0. Importing the TSV text into the Cytoscape software, we could get an ipriflavone-postmenopausal osteoporosis network, as shown in Figure 1(C). This network contained eight nodes and ten edges. In this network, the red nodes had higher degrees, followed by orange and then yellow. The degree rank of them is 4 in CASP3, ESR1, 3 IN CTSK, CYP19A1, ESR2, 1 IN LGMN, BMP4, TNFRSF1A, respectively. This suggested that these genes might be the key or central genes in postmenopausal osteoporosis development.

Molecular docking

The key genes involved in the progression of postmenopausal osteoporosis regulated by ipriflavone are CASP3, ESR1, 3 IN CTSK, CYP19A1, ESR2, 1 IN LGMN, BMP4, TNFRSF1A. The docking scores of this are found in the range of -8.7 to -1.6 kcal/mol. The highest docking score was found in estrogen receptor 2 (-8.7 kcal/mol), followed by ESR1and TNFRSF1A> CYP19A>CASP3>CTSK>LGMN. The interactions and docking

Table 2: Docking scores and 2d interaction of ipriflavone with amino acids of target genes of PMO.

Sl. No.	Gene-ID	Scores	Interactions
1	CASP3	-5.1	TYR 195 (pi-pi stacking), ARG 164, TYR 197 (H bond)
2	ESR2	-8.7	PHE 356 (H bond)
3	CYP19A1	-5.9	PHE 430 (pi-pi stacking)
4	ESR1	-6.4	No interactions
5	LGMN	-1.6	ASN 59 (H bond)
6	TNFRSF1A	-6.4	TRP 314, HIP 248 (pi-pi stacking), Arg 60, HIP 248 (PI cation)
7	CTSK	-2.3	LYS 41 (pi cation)

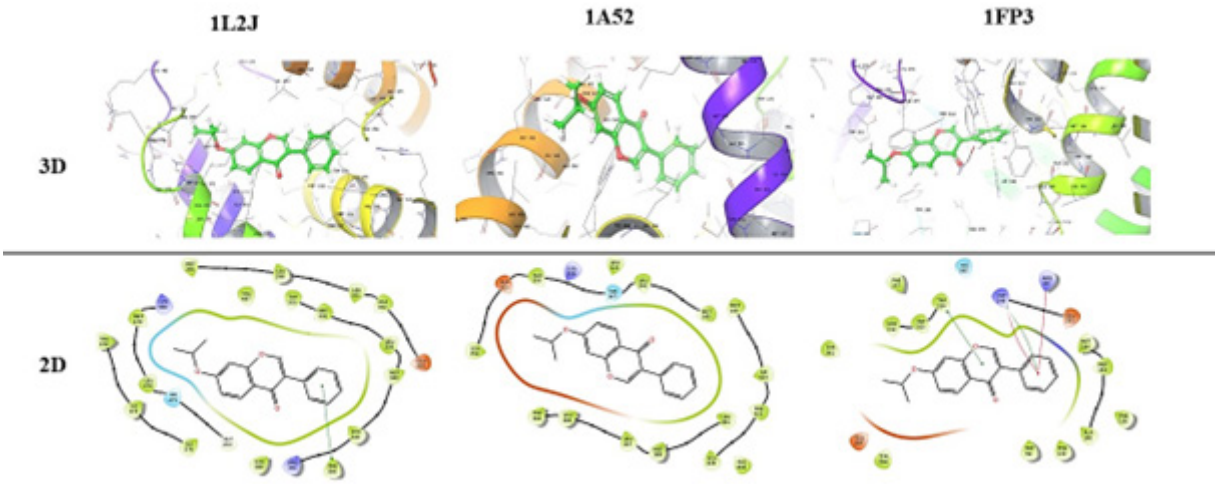

Figure 3: 3D and 2D Interactions of ipriflavone with Human Estrogen Receptor beta (IL2J); Estrogen Receptor Alpha (1A52); N-Acyl-D-Glucosamine 2-Epimerase (1FP3).

scores are given in Table 2, and the 3D and 2D images of the top three scored compounds are depicted in Figure 3.

Molecular dynamic simulation

The MD simulation analysis for RMSD, RMSF, Rg and SASA is depicted in Figure 4. In which Figure 1(A), 1(B), 1(C) is complex RMSD for the backbone (black) and complex (red), the results of 1(A) shows highest fluctuation for backbone and complex in the range of 0.70007864Å and 0.748047 Å respectively, 1(B) highest and lowest is 0.24082 Å, 0.3112189 Å for backbone and complex respectively, for 1(C) highest RMSD fluctuation is seen in the range of 0.3257656 Å for backbone and 0.3829054 Å. The Radius of gyration displayed a fluctuation in the range of 0.15 nm with a decrease at 18 ns, for 1(C), 0.06 nm with 2(C) throughout MD run, and 0.1 nm with 3(C). The solvent-accessible surface area is found in the range of 115 to 140 nm^2, 175 to 194 nm^2, 117-137 nm^2 for 1(D), 2(D), 3(D), respectively, indicating that enough surface is available for the ligand to bind with the protein.

Cytotoxicity

The highest cell viability is observed at a concentration of 25 µg/mL, where the viability is 105.18%. At concentrations lower

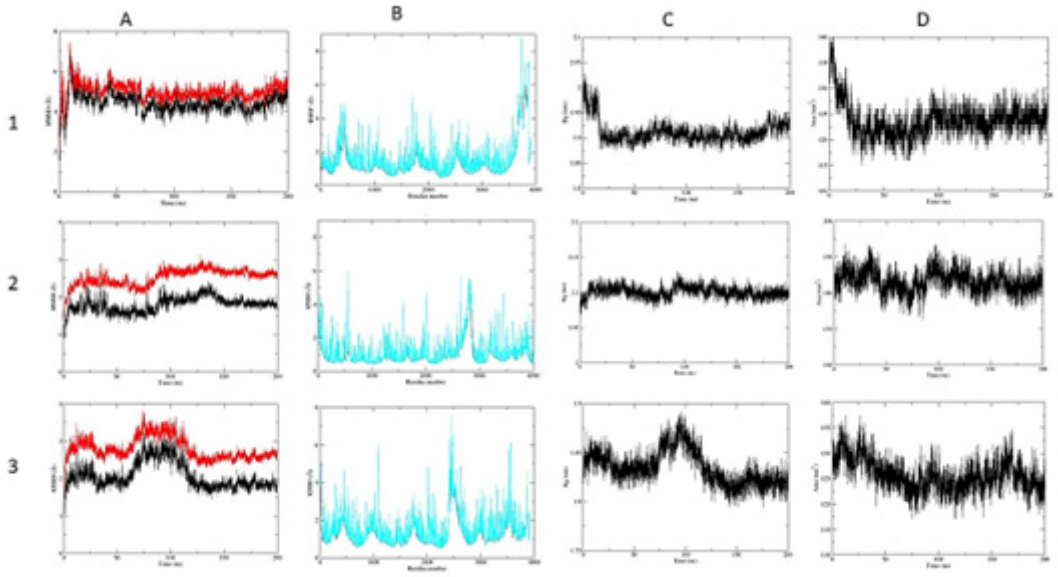

Figure 4: RMSD OF 1(A) 1A52, 2(A) 1FP3, 3(A) 1L2L; RMSF OF 1(B) 1A52, 2(B) 1FP3, 3(B) 1L2L; Radius of gyration 1(C) 1A52, 2(C) 1FP3, 3(C) 1L2L; SASA 1(D) 1A52, 2(D) 1FP3, 3(D) 1L2L.

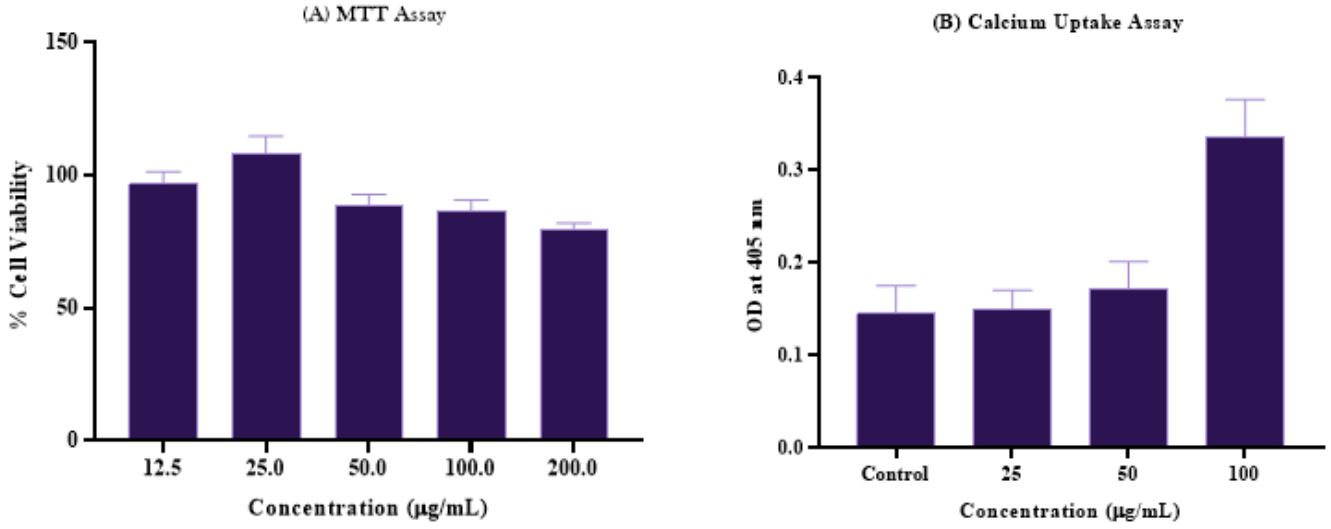

Figure 5: (A) cytotoxicity of ipriflavone by MTT Assay (B) Calcium uptake of ipriflavone. The values are mean±SD (*n*=3).

and higher than 25 µg/mL, the cell viability tends to decrease. Specifically, the cell viability decreases at concentrations of 12.5, 50, 100, and 200 units, with falling values of 96.94%, 88.99%, 86.48%, and 79.77% respectively. The results are represented graphically in the Figure 5.

Calcium uptake assay

These results suggest that the optical density at 405 nm, which correlates with the amount of calcium uptake or mineralisation, increases with increasing concentrations of the substance. The mean OD values show an increasing trend from 0.146 at 0 µg/mL to 0.337 at 100 µg/mL. The Standard Deviation (SD) indicates the variability of the measurements within each concentration group. This data implies that higher concentrations of the substance are associated with increased calcium uptake, as reflected by the higher OD values.

DISCUSSION

In this study, we have screened the activity of ipriflavone against postmenopausal osteoporosis. Protein-protein interaction is a crucial part in predicting the molecular mechanism of disease by importing the common target from drug and disease genes into a string database that provided the degree analysis which revealed that CASP3, ESR1, CTSK AND CYP19A1 play crucial role in the development PMO. The Masco reported that caspase is an important enzyme in cell survival and apoptosis. The reduction in CASP3 can lead to decreased bone mineral density.[34] Estrogen prevents bone loss by inhibiting the synthesis of proinflammatory cytokines by bone marrow and bone cells.[35] Downregulation of CTSK can affect bone resorption by cleaving and removing the organic matrix of type I collagen fibres and CYP19A1 is involved in the formation of estrogen.[36,37]

In molecular docking, ipriflavon was docked with selected target proteins. Amongst Human Estrogen Receptor 2 (IL2J) was found to have maximum binding affinity (-8.7 kcal/mol). The literature suggests that the ESR2 levels are decreased in PMO in women and men compared to premenopausal osteoporosis. Hence, based on the binding affinity of IP with ESR 2, it can predict the possible ESR 2-related activity and manage bone resorption. The interactions of IP with different target proteins revealed that the H bond is formed with amino acids ARG 164, TYR197, PHE 356, and ASN59. Pi-pi bonds with TYR 195, PHE 430, TRP314, and HIP248. These amino acids are responsible for producing stable bonds with IP. The physical behaviour of these docked complexes over time was analysed by MD simulation, which provides valuable insights into the dynamics and structural changes of these molecules. The analysis in Figure 3 focuses on several important parameters: RMSD, RMSF, Rg, and SASA.

RMSD measures the deviation or difference between the positions of atoms in a given structure compared to a reference structure. In this case, the RMSD is calculated for the backbone (black) and the complex (red). In Figure 1(A), the results show that both the backbone and the complex have relatively high fluctuation. The backbone has a fluctuation range of 0.70007864 Å, while the complex exhibits a slightly higher fluctuation with a range of 0.748047 Å. This indicates that both the backbone and the complex are undergoing structural changes during the MD simulation. In Figure 1(B), the highest and lowest RMSD values are provided. The backbone has the highest RMSD value of 0.24082 Å, while the complex has a slightly lower highest RMSD value of 0.3112189 Å. These values give an indication of the maximum structural deviations observed during the simulation. In Figure 1(C), the highest RMSD fluctuations are reported. The backbone shows a fluctuation range of 0.3257656 Å, while the complex has a slightly higher fluctuation range of 0.3829054 Å. These values provide insights into the dynamic behaviour and flexibility of the backbone and the complex. RMSF measures the average fluctuation or mobility of each residue in a protein throughout the simulation. However, the analysis in Figure 3 does not explicitly mention the RMSF values or their interpretation. Including the RMSF analysis would provide a more comprehensive understanding of residue-specific dynamics. The Rg is a measure of the compactness or spatial extent of a biomolecule. It represents the average distance of each atom in a molecule from its centre of mass. Fluctuations in Rg during an MD simulation can provide insights into structural changes and folding/unfolding events. For Figure 1(C), it is stated that there is a fluctuation of 0.15 nm (or 1.5 Å) with a decrease observed at 18 ns. This suggests a conformational change or compaction of the molecule at that specific time point. In 2(C), there is a fluctuation of 0.06 nm (or 0.6 Å) throughout the MD run, indicating relative stability in the size of the molecule. In 3(C), there is a fluctuation of 0.1 nm (or 1.0 Å), which suggests some changes in the compactness but to a lesser extent compared to 1(C). SASA measures the total surface area of a molecule that is accessible to the surrounding solvent molecules. It indicates the available surface area for interactions, such as ligand binding. In Figure 1(D), the SASA range is reported to be between 115 and 140 nm2. In Figure 3(D), the range is between 175 and 194 nm2. Finally, in Figure 3(D), the range is between 117 and 137 nm^2. These values suggest that there is sufficient surface area available for the ligand to bind with the protein throughout the simulation. Overall, the fluctuation patterns observed in RMSD, Rg, and SASA provide insights into the conformational flexibility, compactness, and binding potential of the complex during the simulation.

The cytotoxicity is a major concern in drug development due to the toxic effects of drug molecules, therefore, we have evaluated the *in vivo* cytotoxicity of IP on osteoblast cell lines (MG63). The results depicted that the compound has no toxicity. This indicates that IP is a safe molecule on the osteoblast cell line. Further, the calcium uptake and ALP activity showed a positive effect in calcium deposition as well as cell proliferation *via* ALP hydrolysis inorganic phosphatase, which is a naturally occurring inhibitor

of mineralisation; it also provides inorganic phosphatase for the synthesis of hydroxyl appetite known as the main mineral to give bone structure and density. Hence, this indicates that the IP can be targeted for therapeutic intervention in PMO.

CONCLUSION

In conclusion, this study shows that Ipriflavone (IP) has the potential to be used as a treatment intervention for Postmenopausal Osteoporosis (PMO). Through protein-protein interaction research and molecular docking, IP was discovered to affect critical genes related to PMO, including estrogen receptors. The IP-protein complexes' stability was validated by molecular dynamics analysis. IP-SLN formulations were found to be non-toxic and capable of increasing calcium absorption and promoting osteoblast development *in vitro*. These data suggest IP's potential as an effective treatment for PMO. More study is required to establish IP's biological activity and safety *in vivo*.

ACKNOWLEDGEMENT

The authors are grateful to the Management and the Heads of the NGSM Institute of Pharmaceutical Sciences for providing software, reagents and facilities to carry out this research.

CONFLICT OF INTEREST

The authors declare no conflict of interest in this research work.

ABBREVIATIONS

GO: Gene Ontology; **HRT:** Hormone Replacement Therapy; **OPLS3:** Optimised Potentials for Liquid Simulations-3; **UCSF:** University of California San Francisco; **PMO:** Postmenopausal Osteoporosis; **RMSD:** Root Mean Square Deviation; **RMSF:** Root Mean Square Fluctuation; **SASA:** Solvent Assessable Surface; Area; **ROG:** Radius of Gyration.

REFERENCES

1. Siris ES, Adler R, Bilezikian J, Bolognese M, Dawson-Hughes B, Favus MJ, *et al.* The clinical diagnosis of osteoporosis: A position statement from the National Bone Health Alliance Working Group. Osteoporos Int. 2014;25(5):1439-43. doi: 10.1007/s00198-014-2655-z, PMID 24577348.
2. Marwaha RK, Tandon N, Garg MK, Kanwar R, Narang A, Sastry A, *et al.* Bone health in healthy Indian population aged 50 years and above. Osteoporos Int. 2011;22(11):2829-36. doi: 10.1007/s00198-010-1507-8, PMID 21271341.
3. Sözen T, Özışık L, Başaran NÇ. An overview and management of osteoporosis. Eur J Rheumatol. 2017;4(1):46-56. doi: 10.5152/eurjrheum.2016.048, PMID https://www.ncbi.nlm.nih.gov/pubmed/28293453.
4. Johnell O, Kanis JA. An estimate of the worldwide prevalence and disability associated with osteoporotic fractures. Osteoporos Int. 2006;17(12):1726-33. doi: 10.1007/s00198-006-0172-4, PMID 16983459.
5. Tu KN, Lie JD, Wan CKV, Cameron M, Austel AG, Nguyen JK, *et al.* Osteoporosis: a review of treatment options. P T. 2018;43(2):92-104. PMID 29386866.
6. Papapoulos S, Chapurlat R, Libanati C, Brandi ML, Brown JP, Czerwiński E, *et al.* Five years of denosumab exposure in women with postmenopausal osteoporosis: results from the first two years of the FREEDOM extension. J Bone Miner Res. 2012;27(3):694-701. doi: 10.1002/jbmr.1479, PMID 22113951.
7. Cosman F, Crittenden DB, Adachi JD, Binkley N, Czerwinski E, Ferrari S, *et al.* Romosozumab treatment in postmenopausal women with osteoporosis. N Engl J Med. 2016;375(16):1532-43. doi: 10.1056/NEJMoa1607948, PMID 27641143.
8. Chlebowski RT, Hendrix SL, Langer RD, Stefanick ML, Gass M, Lane D, *et al.* Influence of estrogen plus progestin on breast cancer and mammography in healthy postmenopausal women: the Women's Health Initiative randomized trial. JAMA. 2003;289(24):3243-53. doi: 10.1001/jama.289.24.3243, PMID 12824205.
9. Cummings SR, Eckert S, Krueger KA, Grady D, Powles TJ, Cauley JA, *et al.* The effect of raloxifene on risk of breast cancer in postmenopausal women: results from the MORE randomized trial. Multiple Outcomes of Raloxifene Evaluation. JAMA. 1999;281(23):2189-97. doi: 10.1001/jama.281.23.2189, PMID 10376571.
10. Hu Q, Long C, Wu D, You X, Ran L, Xu J, *et al.* The efficacy and safety of ipriflavone in postmenopausal women with osteopenia or osteoporosis: A systematic review and meta-analysis. Pharmacol Res. 2020;159:104860. doi: 10.1016/j.phrs.2020.104860, PMID 32407952.
11. Civitelli R. *In vitro* and *in vivo* effects of ipriflavone on bone formation and bone biomechanics. Calcif Tissue Int. 1997;61;Suppl 1:S12-4. doi: 10.1007/s002239900378, PMID 9263610.
12. Petilli M, Fiorelli G, Benvenuti S, Frediani U, Gori F, Brandi ML. Interactions between ipriflavone and the estrogen receptor. Calcif Tissue Int. 1995;56(2):160-5. doi: 10.1007/BF00296349, PMID 7736326.
13. Kuiper GGJM, Lemmen JG, Carlsson B, Corton JC, Safe SH, van der Saag PT, *et al.* Interaction of estrogenic chemicals and phytoestrogens with estrogen receptor β. Endocrinology. 1998;139(10):4252-63. doi: 10.1210/endo.139.10.6216, PMID 9751507.
14. Sherman BT, Hao M, Qiu J, Jiao X, Baseler MW, Lane HC, *et al.* David: a web server for functional enrichment analysis and functional annotation of gene lists (2021 update). Nucleic Acids Res. 2022;50(W1):W216-21. doi: 10.1093/nar/gkac194, PMID 35325185.
15. Maurya DK, Sharma D. Evaluation of traditional ayurvedic Kadha for prevention and management of the novel coronavirus (SARS-CoV-2) using *in silico* approach. J Biomol Struct Dyn. 2022;40(9):3949-64. doi: 10.1080/07391102.2020.1852119, PMID 33251972.
16. Mu C, Sheng Y, Wang Q, Amin A, Li X, Xie Y. Potential compound from herbal food of rhizoma Polygonati for treatment of COVID-19 analyzed by network pharmacology: viral and cancer signaling mechanisms. J Funct Foods. 2021;77:104149. doi: 10.1016/j.jff.2020.104149, PMID 32837538.
17. Szklarczyk D, Gable AL, Nastou KC, Lyon D, Kirsch R, Pyysalo S, *et al.* The STRING database in 2021: customizable protein-protein networks, and functional characterization of user-uploaded gene/measurement sets. Nucleic Acids Res. 2021;49(D1):D605-12. doi: 10.1093/nar/gkaa1074, PMID 33237311.
18. Hamzah SN, Avicor SW, Alias Z, Razak SA, Bakhori SKM, Hsieh TC, *et al. In vivo* glutathione S-transferases Superfamily Proteome Analysis: an Insight into *Aedes albopictus* Mosquitoes upon Acute Xenobiotic Challenges. Insects. 2022;13(11). doi: 10.3390/insects13111028, PMID 36354852.
19. Doncheva NT, Morris JH, Gorodkin J, Jensen LJ. Cytoscape StringApp: network analysis and visualization of proteomics data. J Proteome Res. 2019;18(2):623-32. doi: 10.1021/acs.jproteome.8b00702, PMID 30450911.
20. Huang DW, Sherman BT, Lempicki RA. Systematic and integrative analysis of large gene lists using David bioinformatics resources. Nat Protoc. 2009;4(1):44-57. doi: 10.1038/nprot.2008.211, PMID 19131956.
21. Sheikh IA, Jiffri EH, Ashraf GM, Kamal MA, Beg MA. Structural studies on inhibitory mechanisms of antibiotic, corticosteroid and catecholamine molecules on lactoperoxidase. Life Sci. 2018;207:412-9. doi: 10.1016/j.lfs.2018.06.027, PMID 29953881.
22. Sherman BT, Hao M, Qiu J, Jiao X, Baseler MW, Lane HC, *et al.* David: a web server for functional enrichment analysis and functional annotation of gene lists (2021 update). Nucleic Acids Res. 2022;50(W1):W216-21. doi: 10.1093/nar/gkac194, PMID 35325185.
23. Das SK, Mahanta S, Tanti B, Tag H, Hui PK. Identification of phytocompounds from Houttuynia cordata Thunb. as potential inhibitors for SARS-CoV-2 replication proteins through GC–MS/LC–MS characterization, molecular docking and molecular dynamics simulation. Mol Divers. 2022;26(1):365-88. doi: 10.1007/s11030-021-10226-2, PMID 33961167.
24. Joseph Sahayarayan J, Soundar Rajan K, Nachiappan M, Prabhu D, Guru Raj Rao R, Jeyakanthan J, *et al*. Identification of potential drug target in malarial disease using molecular docking analysis. Saudi J Biol Sci. 2020;27(12):3327-33. doi:10.1016/j.sjbs.2020.10.019.
25. Kalirajan R, Sankar S, Jubie S, Gowramma B. Molecular docking studies and in-silico ADMET screening of some novel oxazine substituted 9-anilinoacridines as topoisomerase II inhibitors. Indian J Pharm Educ Res. 2017;51(1):110-5. doi: 10.5530/ijper.51.1.15.
26. Chaudhari HK, Pahelkar AR. 3D QSAR, Docking, Molecular dynamics simulations and MM-GBSA studies of Extended Side Chain of the Antitubercular Drug;6S: 2-Nitro-6-{[4-(trifluoromethoxy) benzyl] oxy}-6,7-dihydro-5H-imidazo[2,1-b] [1,3] oxazine. Infect Disord Drug Targets. 2018;18. doi:10.2174/1871526518666181015145545.
27. Baildya N, Khan AA, Ghosh NN, Dutta T, Chattopadhyay AP. Screening of potential drug from *Azadirachta indica* (Neem) extracts for SARS-CoV-2: an insight from molecular docking and MD-simulation studies. J Mol Struct. 2021; 1227:129390. doi: 10.1016/j.molstruc.2020.129390, PMID 33041371.
28. Sharma S, Deep S. In-silico drug repurposing for targeting SARS-CoV-2 main protease (Mpro). J Biomol Struct Dyn. 2022;40(7):3003-10. doi: 10.1080/07391102.2020.1844058, PMID 33179568.
29. Kumar D, Kumari K, Jayaraj A, Kumar V, Kumar RV, Dass SK, *et al.* Understanding the binding affinity of noscapines with protease of SARS-CoV-2 for COVID-19 using MD

simulations at different temperatures. J Biomol Struct Dyn. 2021;39(7):2659-72. doi: 10.1080/07391102.2020.1752310, PMID 32362235.

30. Suresh P, Xavier AS, Karthik VP, Punnagai K. Anticancer activity of *Cissus quadrangularis* l. Methanolic extract against MG63 Human osteosarcoma cells – an *in vitro* evaluation using cytotoxicity assay. Biomed Pharmacol J. 2019;12(2):975-80. doi: 10.13005/bpj/1724.
31. Packialakshmi B, Sowndriya SR. Anti-cancer effect of *Gymnema sylvestre* leaf extract against MG63, human osteosarcoma cell line - an *in vitro* analysis. Int J Curr Res Rev. 2019;11(11):18-24. doi: 10.31782/IJCRR.2019.11114.
32. Sadhasivam G, Kulanthai K, Natarajan A. Synthesis and anti-cancer studies of 2, 6-disubstituted benzothiazole derivatives. Orient J Chem. 2015;31(2):819-26. doi: 10.13005/ojc/310224.
33. Matinfar M, Mesgar AS, Mohammadi Z. Evaluation of physicochemical, mechanical and biological properties of chitosan/carboxymethyl cellulose reinforced with multiphasic calcium phosphate whisker-like fibers for bone tissue engineering. Mater Sci Eng C Mater Biol Appl. 2019;100:341-53. doi: 10.1016/j.msec.2019.03.015, PMID 30948070.
34. Miura M, Chen XD, Allen MR, Bi Y, Gronthos S, Seo BM, *et al.* A crucial role of caspase-3 in osteogenic differentiation of bone marrow stromal stem cells. J Clin Invest. 2004;114(12):1704-13. doi: 10.1172/JCI20427, PMID 15599395.
35. Pacifici R. Editorial: cytokines, estrogen, and postmenopausal osteoporosis - the second decade. Endocrinology. 1998;139(6):2659-61. doi: 10.1210/en.139.6.2659.
36. Song ZH, Xie W, Zhu SY, Pan JJ, Zhou LY, He CQ. Effects of PEMFs on Osx, Ocn, TRAP, and CTSK gene expression in postmenopausal osteoporosis model mice. Int J Clin Exp Pathol. 2018;11(3):1784-90. PMID 31938285.
37. Ma HJ, Fu SC, Xiao A, Cai WK, Wang P, Shen ML, *et al.* The associations of CYP19A1 rs700518 polymorphism with bone mineral density and risk of osteoporosis: a meta-analysis. Gynecol Endocrinol. 2020;36(7):626-31. doi: 10.1080/09513590.2020.1727431, PMID 32070153.

Cite this article: John A, Ashtekar H, Gupta D, Narayanan AV, Kumar P. Mechanistic Insights into Ipriflavone's Role in Postmenopausal Osteoporosis through Integrated Computational and *in vitro* Techniques. J Young Pharm. 2023;15(4):629-37.